Simulation of Shielding Options for an Active Collimator System

Christopher Gauthier* and R.T. Jones†

University of Connecticut

(Dated: March 14, 2003)

Abstract

This paper covers the details of a simulation of three shielding options for an active collimator system to be used in the upcoming GlueX experiment. The simulations were run with *Geant*, a high-energy particle physics simulation program developed at CERN. Three collimator shielding options, heavy, moderate and light shielding, were simulated. The simulations revealed that the light shielding option was the least effective in blocking secondary particles from penetrating into the experimental hall while the heavy and moderate shielding options both provided adequate shielding for the collimator. The heavy and moderate shielding options lead to acceptable background levels in the detectors; however, cost and ease of construction make the moderate shielding option the more desirable of the two.

INTRODUCTION

The GlueX Experiment will test our current picture of the subatomic world. The force between quarks is thought to be caused by a nuclear field called "glue". Although the properties of the glue are well understood where the field is weak, inside the nucleus where this field is quite strong its properties are largely unknown. In the GlueX experiment, a beam of high energy gamma rays will excite this glue, thereby revealing its physical properties.

The GlueX experiment will rely on the use of high energy gamma rays to probe the internal structure of the bond between quarks. Linearly polarized gamma rays have preferential angles of emission for different final states, which aids in the partial-wave analysis of the final state. Using a beam of linearly polarized gamma rays in the GlueX experiment will improve the precision of the results.

The Coherent Bremsstrahlung process creates a beam of gamma rays with a degree of linear polarization that is dependent on the angle of radiation. This angular dependence can be used to select and remove the unpolarized component of the gamma ray beam. A collimator can absorb a significant amount of the unpolarized gamma rays, while leaving the polarized component unaffected.

Increasing the polarization of the gamma rays through collimation has the adverse effect of decreasing the total flux reaching the target. It has been determined that collimating the beam to 40% polarization will reduce the flux to 20% [1], with 80% of the beam's total power absorbed by the collimator. The process of collimation has the disadvantage of creating copious amounts of unwanted secondary particles. This experiment will use a charged particle track detector that is sensitive to low energy particles; therefore, effective shielding for the collimator is necessary to keep any background from interfering with the performance of this detector.

Three different shielding scenarios for the collimator system have been designed. For each design, a simulated beam of coherent bremsstrahlung photons passed through the collimator and the flux of secondary particles reaching the tracker was measured. The results for each design were compared with each other and with the cosmic ray background levels to determine which option worked the best at shielding the tracker from secondary particles.

SOFTWARE

The simulation was carried out using *Geant*, a physics simulation program developed at CERN [2]. *Geant* simulates the passage of high-energy particles through matter using the Monte Carlo technique. The program uses a random number sequence to assign each particle a unique track history based on known interaction probabilities. For example, as a photon traverses a given material, for each type of physical process that photons can undergo in that medium, a "length until interaction" is calculated, with a probability of occurrence given by the exponential distribution whose average is determined by the cross section. The process with the shortest "length until interaction" will be the process that takes place. A similar procedure determines the types and four momenta of the final particles produced by the interaction.

The original *Geant* release includes many of the common processes that occur in high-energy particle physics. Some interactions that are important in this analysis are not included in the standard *Geant* release. These include photo-hadronic interactions and muon pair production. Art Snyder from SLAC has created a *Geant* plugin package called *Gelhad* [3] that simulates the photoproduction of neutrons, protons, alpha particles, and pions. To simulate the production of muon pairs by photons, the electron-positron pair production package *Gpairg* was modified to convert a fraction of the electron-positron pairs into muon pairs, which are then generated according to the kinematics appropriate for muons. The fraction of electron positron pairs lost by this algorithm is on the order of $(m_e/m_\mu)^2 = 2.34\times10^{-5}$, therefore the depletion in the electron positron yield is negligible.

Seven virtual detector volumes named DET1 through DET7 are placed in the simulated GlueX geometry in areas that are of the most interest. Each time a particle passes through any one of these virtual detectors the particle's position, momentum, energy and species are recorded in one of seven ntuples, one ntuple for each virtual detector. This system cuts down on the amount of disk space that a completed simulation uses, and allows for quicker access to data. The placement of the virtual detectors in the simulated GlueX environment is shown in Fig. 1.

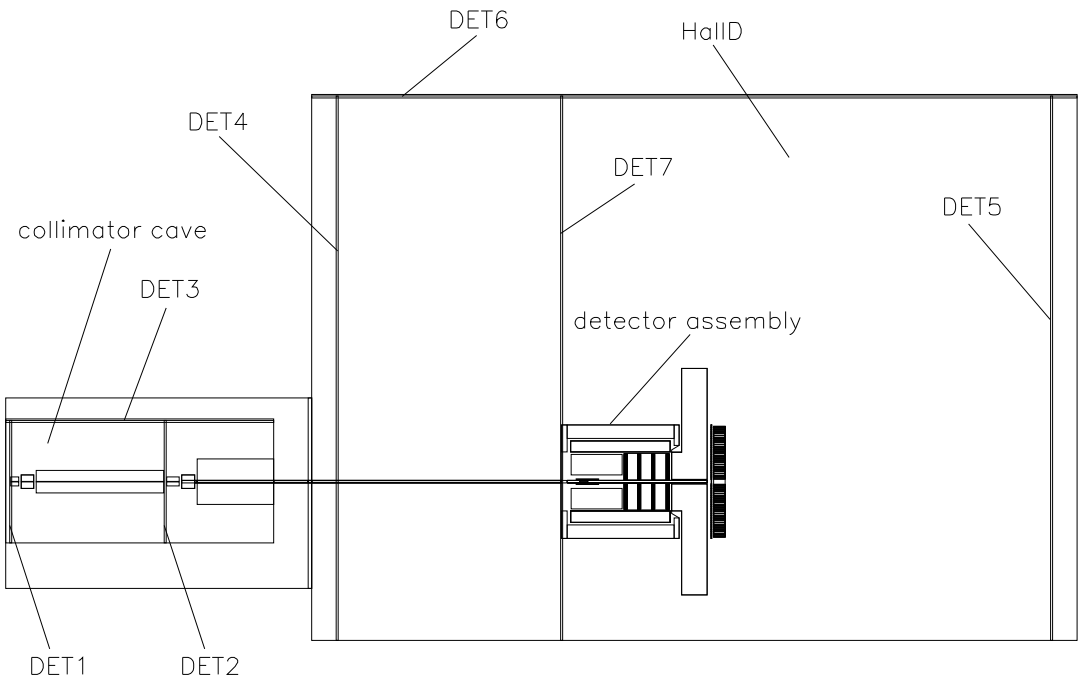

FIG. 1: Placement of the virtual detectors in the simulated GlueX environment. Virtual detector placement is the same for all three shielding options

The static properties of the GlueX experimental volume, which includes the design parameters for the collimator system and the detector assembly, are stored in HDDS, an XML-based geometry specification [4]. In HDDS, the geometry of a virtual object is declared by the user in an XML file by the use of XML tags. For example, the tag

```
<box name="BOX1" X_Y_Z="10.0  10.0  10.0" material="Air"/>
```

creates a box in *Geant* named BOX1 with dimensions 10.0 cm by 10.0 cm by 10.0 cm and is filled with air. The tag

```
<composition name="CompBox" envelope="MBOX">
   <posXYZ volume="BOX1" X_Y_Z="0.0  0.0  0.0" />
</composition>
```

positions BOX1 at the origin of a mother volume MBOX and then declares the composite

volume as CompBox. Each subsystem of GlueX has its own XML file description, and these are linked and converted into a FORTRAN file using a program hdds-geant.

THREE SCENARIOS

The basic collimator system itself is composed of two separate stages. When the gamma rays reach the first (primary) collimator, rays that left the source at large enough angles are absorbed on the collimator face while allowing gamma rays with low emission angles to pass through unscathed. The polarization of gamma rays created through Coherent Bremsstrahlung depend sensitively on the emission angle; therefore highly polarized gamma rays will pass through the collimator, while unpolarized gamma rays will be preferentially absorbed on the collimator face. To remove the shower fragments produced in the primary collimator, a sweeping magnet with a strength of 0.4 T·m is placed after the primary collimator along with a large iron absorber to stop charged particles. This sequence is repeated a second time in the secondary collimator. Simulations of three shielding scenarios were run; each incorporating the same basic two-collimator design. The shielding designs have been designated as heavy, moderate and light, to distinguish between their levels of shielding. The dimensions of the hall are the same as given in the most recent blueprints of Hall D.

Heavy Shielding Scenario

The Heavy shielding option shown in Fig. 2 utilizes sufficient shielding to stop essentially all particles produced by collimation. The collimator assembly is encased inside a thick concrete shield that is at its thinnest 50 cm and at its thickest 100 cm. The iron absorbers in front of the first and second sweeping magnets are 5.0 m and 3.0 m long, respectively. A lead wall with dimensions $5.5 \times 4.2 \times .15$ m^3 is placed upstream from the entire collimator assembly for additional shielding. The dimensions of the heavy shielded collimator components and their placement relative to the detector assembly are shown in Table I.

Moderate Shielding Scenario

The moderate shielding option shown in Fig. 3 is a variation of the heavy shielding

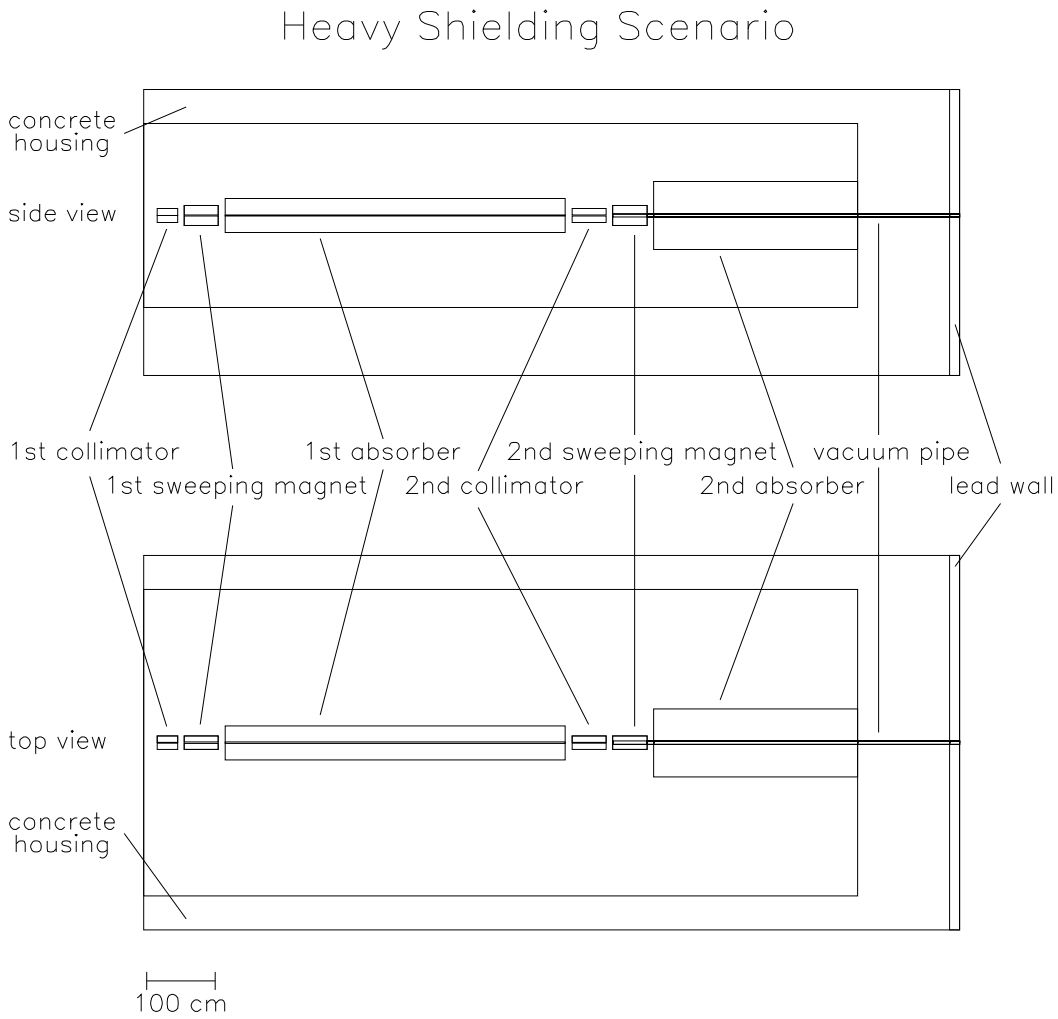

FIG. 2: Diagram of the heavily shielded collimator

scenario. The front of the concrete shield has been reduced to a thickness of 35 cm and the lead plate has been reduced in size to the dimensions $4.7\times2.9\times.15$ m^3. To compensate for this loss in shielding , two large concrete blocks are placed downstream from the first and second absorbers. Both absorbers are shorter in this shielding version. The first absorber is now 2.0 m in length and the second absorber is now 1.0 m in length. The design parameters for the moderate shielding option are shown in Table II.

TABLE I: Dimensions of the heavily shielded collimator components.

Component (shape: cubic)	Material	Width (cm)	Height (cm)	Length (cm)	Distance from detector assembly (cm)
concrete housing	concrete	550	420	1200	na
inner collimator cave	air	450	270	1050	na
first sweeping magnet	iron	20	30	50	2070
first absorber	iron	50	50	500	1560
second sweeping magnet	iron	20	30	50	1440
second absorber	iron	100	100	300	1130
lead wall	lead	550	420	15	980

Component (shape: cylindrical)	Material	r_{in} (cm)	r_{out} (cm)	Length (cm)	Distance from detector assembly (cm)
primary collimator	tungsten	0.25	10	30	2130
secondary collimator	nickel	0.50	10	50	1500
vacuum pipe	iron	2.2	2.5	1488	na

Light Shielding Scenario

The light shielding option shown in Fig. 4 is a further reduction of the heavy shielding option. The lead plate is now $4.5\times2.7\times.15$ m^3 and is inside the concrete shield just downstream of the second absorber. The first and second iron absorbers are 2.0 m and 1.0 m in length, respectively. As in the moderate shielding design, the concrete shield is thinner than in the heavy shielding option. Here the concrete in the front of the collimator cave is 35 cm. The design parameters for this scenario are shown in Table III.

RESULTS

Simulations of each of these designs were run starting with 30 million original photons produced through a coherent bremsstrahlung generator. This corresponds to 7.0 ms of run time at 1.0 μA of electron beam current on a diamond radiator of 15 μm thickness a

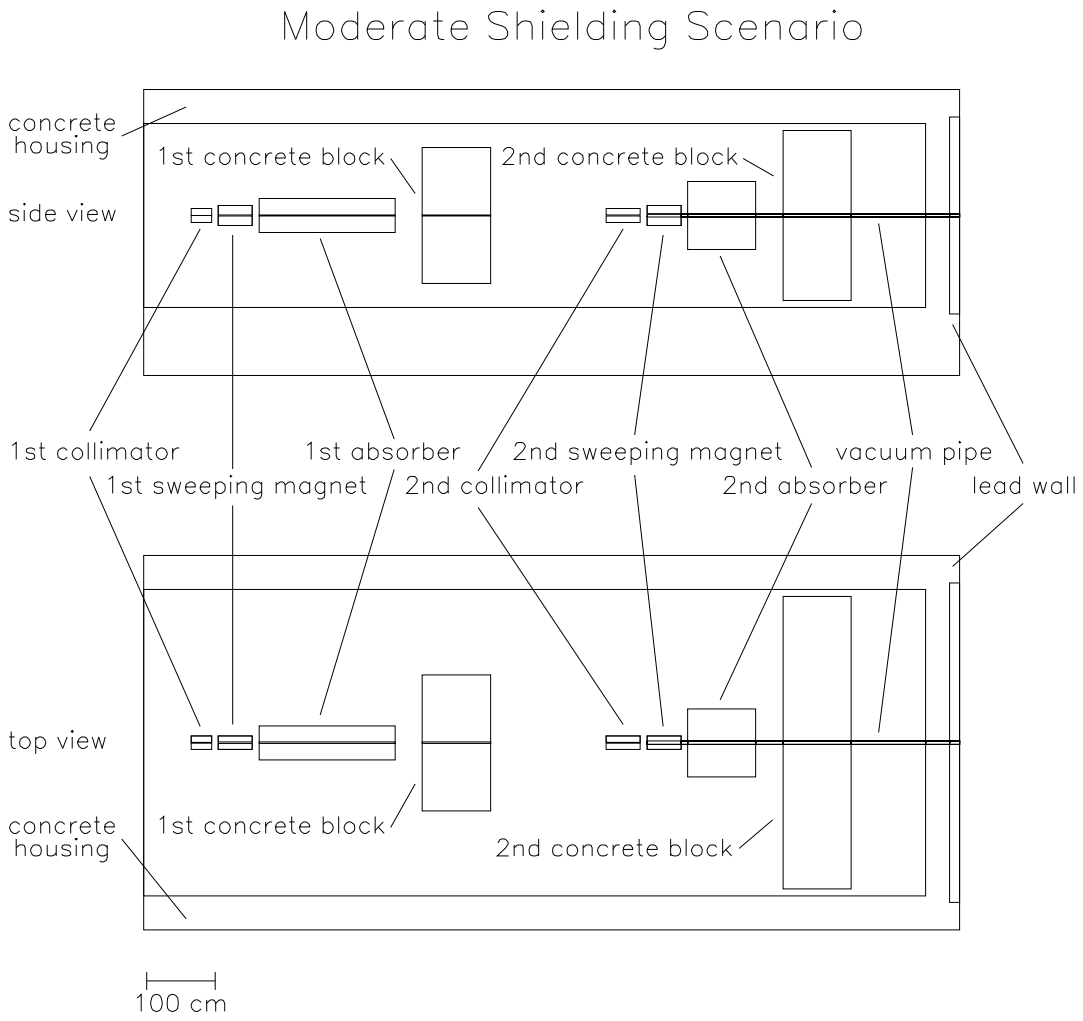

FIG. 3: Diagram of the moderately shielded collimator

distance 75 m upstream of the primary collimator. The simulation was used to measure the flux as a function of the radial distance from the beam line for photons, electron-positron pairs, neutrons, and muon pairs at DET7. The charged particle tracker, shown in Fig. 5, is sensitive to low energy charged particles. Therefore an analysis of the background levels of electrons, positrons, and muons in the central tracker will be an important factor in determining the best shielding option. Only particles with a radial distance greater than 5 cm from the beam axis were included in this analysis since this is the inner radius of the barrel drift chamber. The fraction of counts seen in the tracker due to background is given by $(1\text{-}e^{-B\cdot\delta t})$, where B is the average number of background particles entering the tracker per

TABLE II: Dimensions of the moderately shielded collimator components.

Component (shape: cubic)	Material	Width (cm)	Height (cm)	Length (cm)	Distance from detector assembly (cm)
concrete housing	concrete	550	420	1200	na
inner collimator cave	air	450	270	1150	na
first sweeping magnet	iron	20	30	50	2020
first absorber	iron	50	50	200	1810
first concrete block	concrete	200	200	100	1670
second sweeping magnet	iron	20	30	50	1390
second absorber	iron	100	100	100	1280
second concrete block	concrete	430	250	100	1140
lead wall	lead	550	420	15	980

Component (shape: cylindrical)	Material	r_{in} (cm)	r_{out} (cm)	Length (cm)	Distance from detector assembly (cm)
primary collimator	tungsten	0.25	10	30	2080
secondary collimator	nickel	0.50	10	50	1500
vacuum pipe	iron	2.2	2.5	1438	na

unit time and δt is the shutter time of the tracker, which is roughly equal to 150 ns. After several simulations, it was discovered that the background could be significantly reduced with the placement of a vacuum pipe that extends from the face of the second sweeping magnet to the entrance of the GlueX detector assembly. The vacuum pipe in all simulations was made of an iron tube 3 mm thick and was closed at both ends by a plastic Mylar cap that was 0.5 mm thick. Study of different arrangements of the collimator components showed that the background flux depends on the placement of the secondary collimator. This is probably caused by the variation in the distance between the secondary collimator and the lead wall exit aperture, which defines the solid angle of the secondary collimator that is visible by line-of-sight from inside the hall. Analysis of the background flux led to the conclusion that much of the background is emitted at small angles; therefore much emphasis was put on shielding the front of the collimator cave.

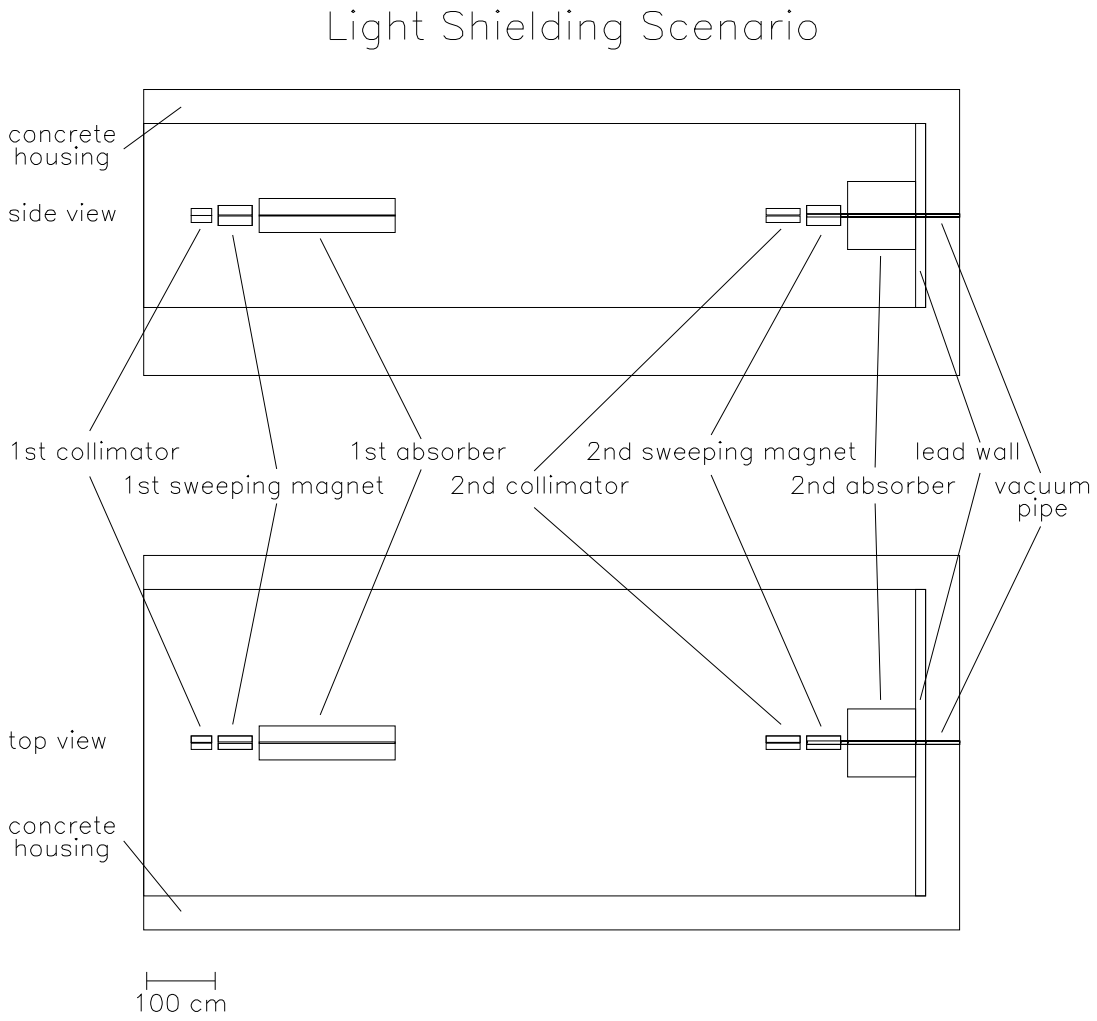

FIG. 4: Diagram of the lightly shielded collimator

Heavy Shielding

Fig. 6 and Table IV show the results of the heavy shielding option. The heavy shielding scenario had the lowest total flux of all the shielding options. The rate of charged secondary particles entering the tracker was comparable to the rate of cosmic rays entering the tracker. The muon flux was very small relative to the electron-positron flux and was not a significant component of the total background reaching the tracker. The flux as a function of radius decreases quickly as the radial distance increases. This indicates that there is sufficient shielding in the exit wall of the collimator cave.

TABLE III: Dimensions of the lightly shielded collimator components.

Component (shape: cubic)	Material	Width (cm)	Height (cm)	Length (cm)	Distance from detector assembly (cm)
concrete housing	concrete	550	420	1200	na
inner collimator cave	air	450	270	1150	na
first sweeping magnet	iron	20	30	50	2020
first absorber	iron	50	50	200	1810
second sweeping magnet	iron	20	30	50	1155
second absorber	iron	100	100	100	1045
lead wall	lead	450	270	15	1030

Component (shape: cylindrical)	Material	r_{in} (cm)	r_{out} (cm)	Length (cm)	Distance from detector assembly (cm)
primary collimator	tungsten	0.25	10	30	2080
secondary collimator	nickel	0.50	10	50	1215
vacuum pipe	iron	2.2	2.5	1203	na

TABLE IV: Background rates for the heavy shielding option.

particle type	background rate in barrel DC (s^{-1})	background occupation fraction in barrel DC	total background through DET7 (s^{-1})
photons	$(9.52\pm0.12)\times10^{5}$	0.133 ± 0.002	$(1.05\pm0.003)\times10^{7}$
e^- e^+	$(8.03\pm0.34)\times10^{4}$	$(1.20\pm0.05)\times10^{-2}$	$(5.02\pm0.09)\times10^{5}$
neutrons	$(1.19\pm0.13)\times10^{4}$	$(2.0\pm0.2)\times10^{-3}$	$(8.60\pm0.35)\times10^{4}$
μ^- μ^+	$(2.60\pm0.61)\times10^{3}$	$(4.0\pm0.9)\times10^{-4}$	$(1.33\pm0.14)\times10^{4}$
total	$(1.05\pm0.01)\times10^{6}$	(0.145 ± 0.002)	$(1.11\pm0.004)\times10^{7}$

Moderate Shielding

The background flux in the moderate shielding option, as shown in Fig. 7 and Table V , was very close to the levels in the heavy shielding option. There were only slight increases

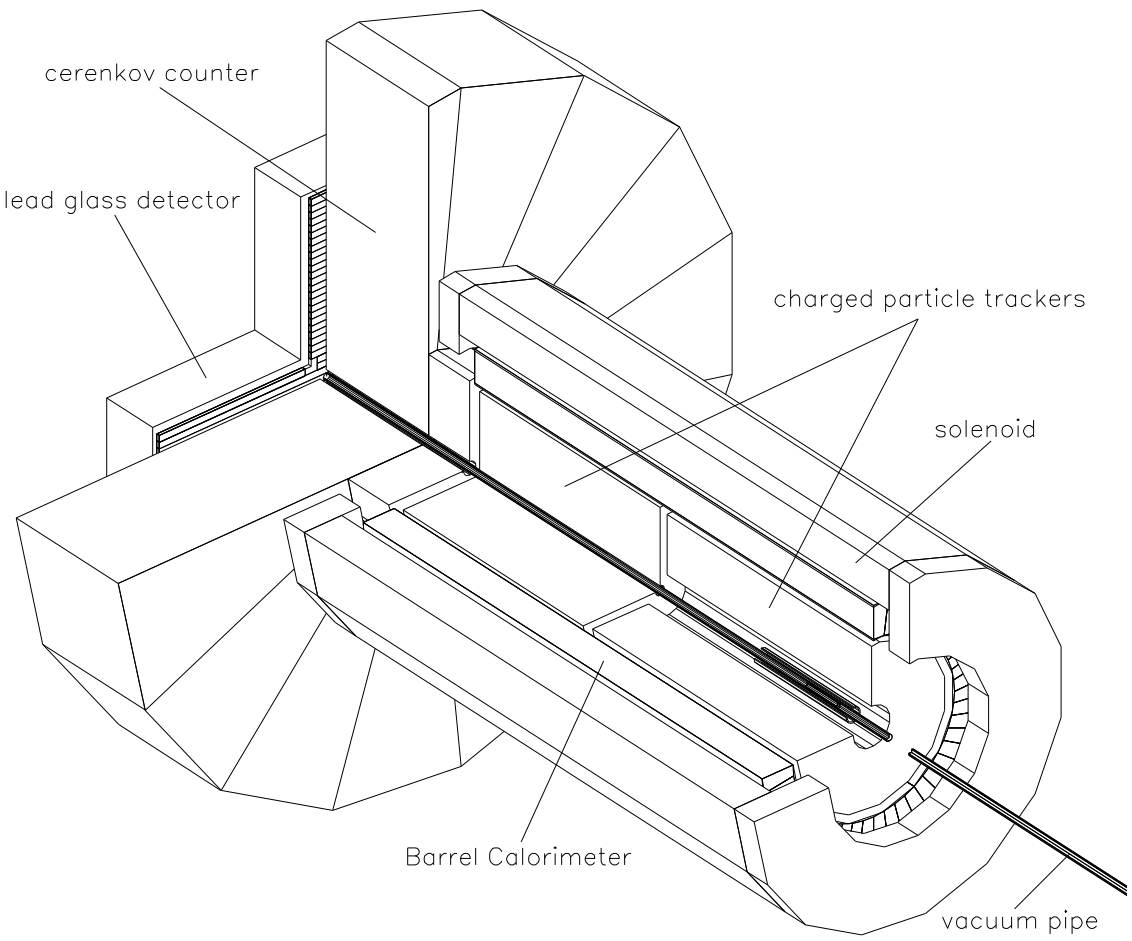

FIG. 5: Diagram of the GlueX detector assembly

TABLE V: Background rates for the moderate shielding option.

particle type	background rate in barrel DC (s^{-1})	background occupation fraction in barrel DC	total background through DET7 (s^{-1})
photons	$(9.07\pm0.11)\times10^{5}$	0.127 ± 0.002	$(1.09\pm0.004)\times10^{7}$
e^- e^+	$(7.30\pm0.32)\times10^{4}$	$(1.1\pm0.05)\times10^{-2}$	$(5.91\pm0.09)\times10^{5}$
neutrons	$(9.00\pm1.13)\times10^{3}$	$(1.35\pm0.17)\times10^{-3}$	$(6.70\pm0.31)\times10^{4}$
μ^- μ^+	$(4.43\pm0.80)\times10^{3}$	$(6.64\pm1.19)\times10^{-4}$	$(1.53\pm0.15)\times10^{4}$
total	$(9.93\pm0.12)\times10^{5}$	0.138 ± 0.002	$(1.16\pm0.004)\times10^{7}$

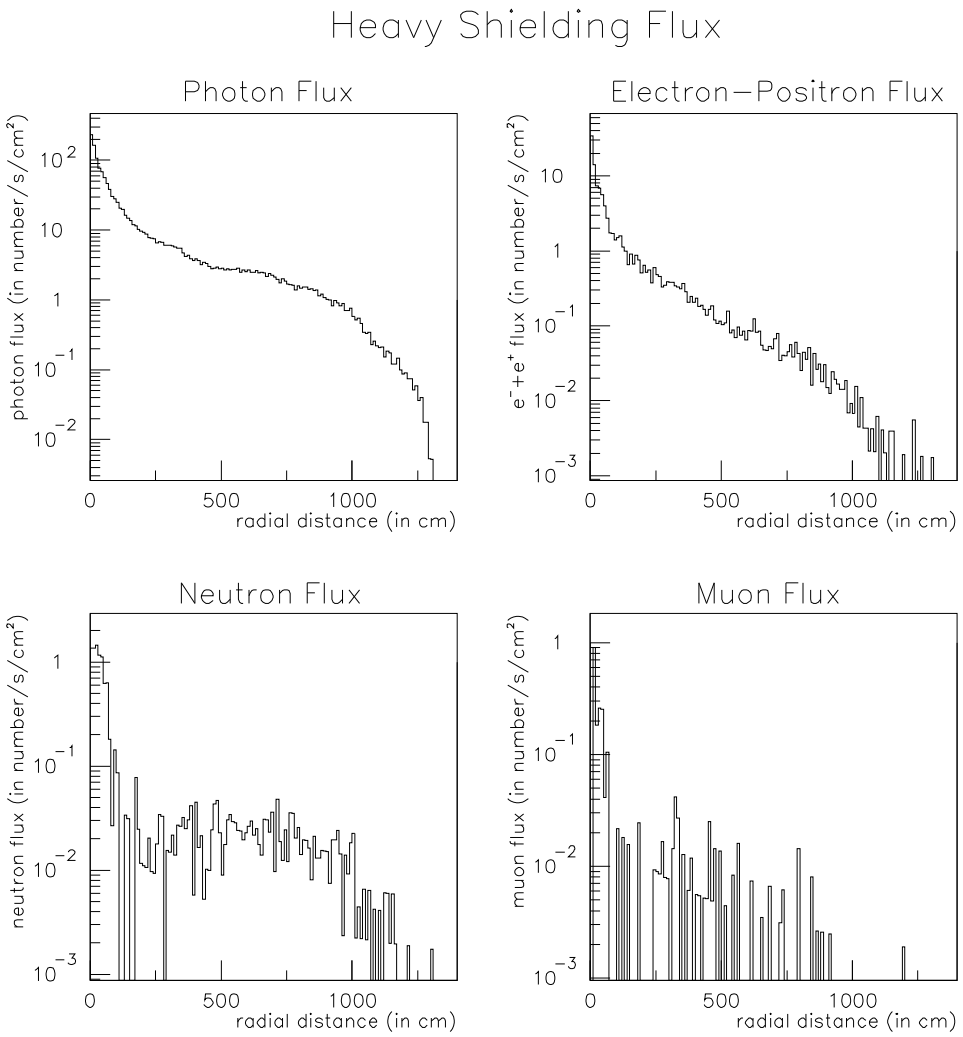

FIG. 6: Graphs of the flux near the detector assembly for various particles with the heavy shielding option

from the heavy shielding option in the background levels of the electrons, photons and muons and a decrease in the neutron flux. The decrease in neutron flux is a result of the two concrete blocks behind the iron absorbers, which absorb neutrons. From the background rates at the tracker given in Tables 4 and 5, it is clear that the moderate shielding option is better at shielding the tracker than the heavy shielding option, which is again a result of the two concrete blocks.

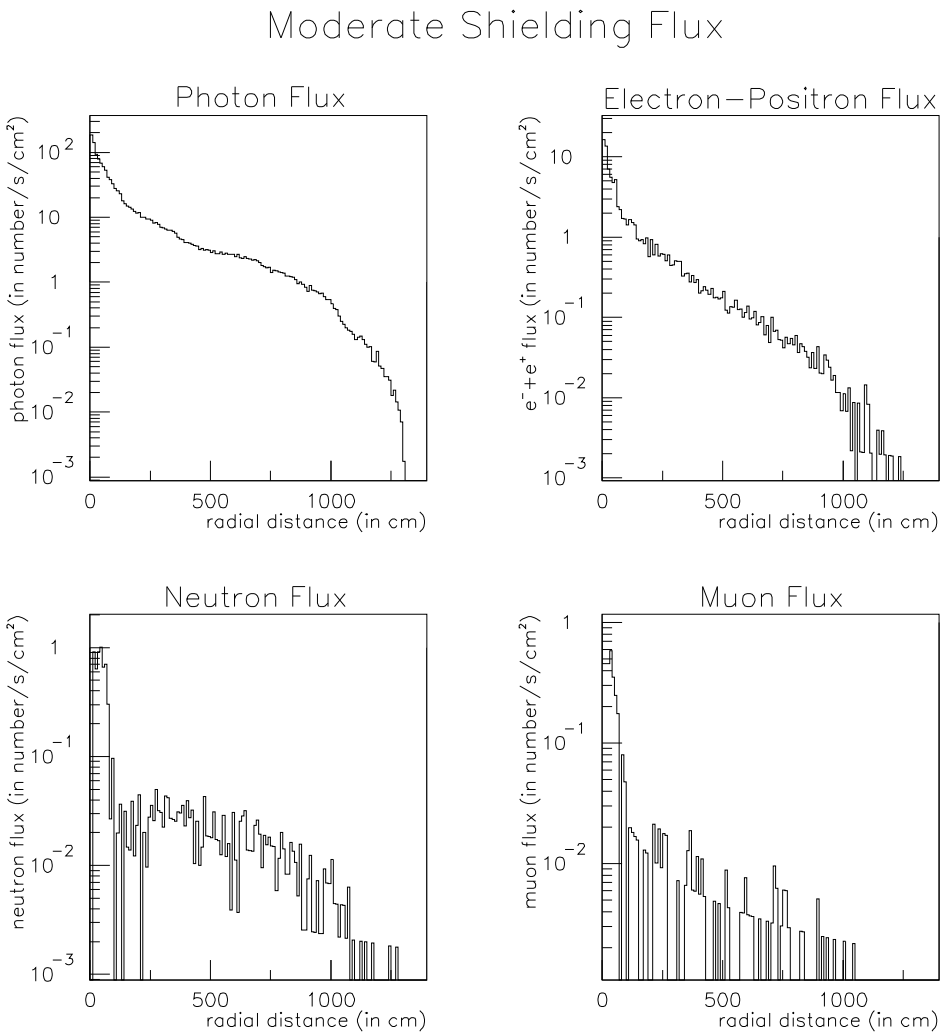

FIG. 7: Graphs of flux near the detector assembly for various particles with the moderate shielding option

Light Shielding

As indicated in Fig. 8 and Table VI , there was a big increase in the flux levels for all particle types in the light shielding option. Particle fluxes increased by one to two orders of magnitude. This significant increase in flux is not only the result of a reduction in the shielding but is also the result of the placement of the secondary collimator at the downstream end of the cave. The decrease in the flux as a function of radius is considerably slower in this scenario, which indicates a lack of shielding at the exit of the collimator cave.

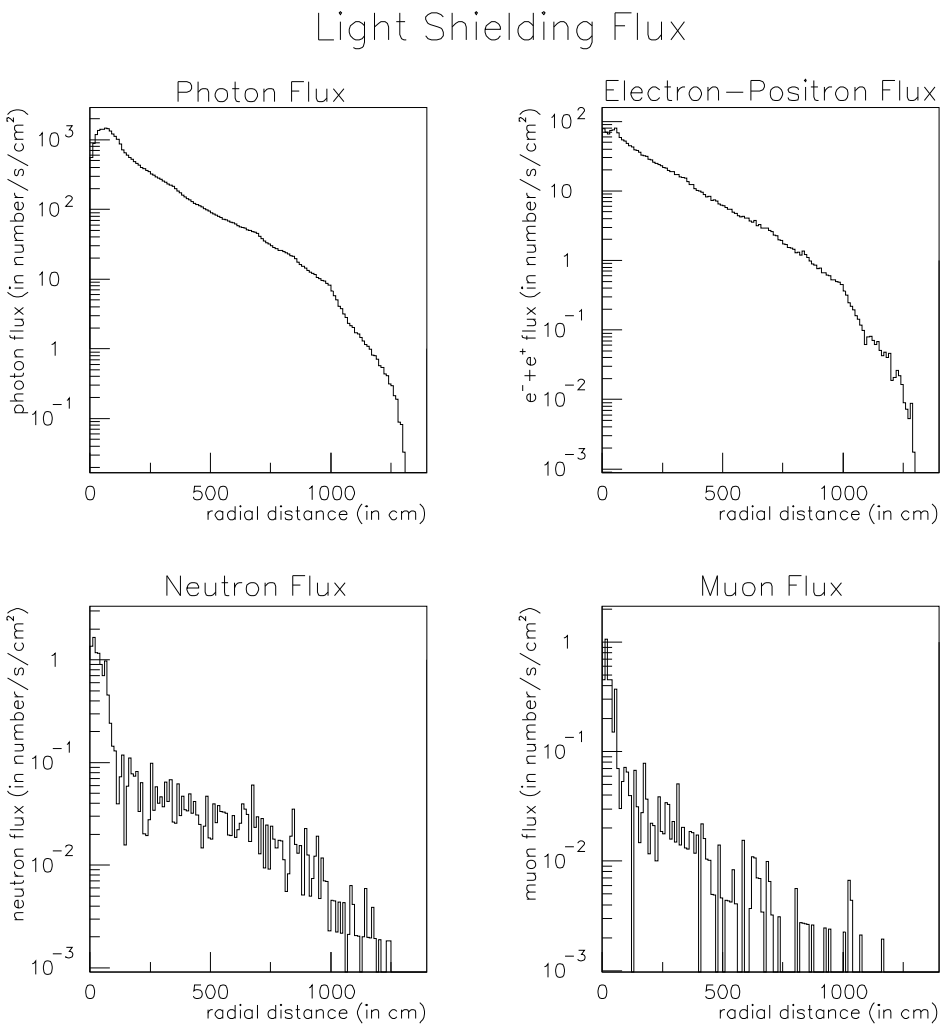

FIG. 8: Graphs of flux near the detector assembly for various particles with the light shielding option

CONCLUSION

These simulated collimators do not take into account all aspects of a real active collimator system. The simulations do not take into account an access tunnel into the collimator housing, which could change the background levels in the hall. However, an access tunnel could be designed that would allow a minimum of radiation to escape from the cave into the hall. Other components of the collimator system that were left out of the simulation were fixtures to hold the collimator components in place, and a flux monitor inside the primary

TABLE VI: Background rates for the light shielding option.

particle type	background rate in barrel DC (s^{-1})	background occupation fraction in barrel DC	total background through DET7 (s^{-1})
photons	$(1.47\pm0.005)\times10^{7}$	0.890 ± 0.003	$(3.15\pm0.002)\times10^{8}$
e^- e^+	$(8.45\pm0.11)\times10^{5}$	0.119 ± 0.002	$(1.93\pm0.005)\times10^{7}$
neutrons	$(1.14\pm0.13)\times10^{4}$	$(1.71\pm0.19)\times10^{-3}$	$(1.01\pm0.04)\times10^{5}$
μ^- μ^+	$(4.57\pm0.81)\times10^{3}$	$(7.00\pm1.24)\times10^{-4}$	$(2.60\pm0.19)\times10^{4}$
total	$(1.56\pm0.005)\times10^{7}$	(0.903 ± 0.003)	$(3.34\pm0.002)\times10^{8}$

collimator to help position the collimator on the beam line. These components were seen as irrelevant to this study since little of the initial gamma ray beam flux would be absorbed by these components. The photo-hadronic interaction generator *Gelhad*, which was used in this simulation, should be checked against other hadronic generators to confirm *Gelhad's* reliability. Muon-nuclear interactions were not included in this study, since it is a negligible second order effect. The electromagnetic generator in *Geant* is well tested and has proved itself reliable.

From this study, the light shielding option does not have enough shielding to stop a large amount of the background produced in the collimator. Therefore, the light shielding scenario would not be the most desirable option. The differences in the flux between the heavy and moderate shielding scenarios were negligible. The moderate shielding scenario would be more cost effective and easier to manufacture than the heavy shielding option and this coupled with low background levels at the detector assembly make the moderate shielding option the best of the three scenarios.

* gauthier@phys.uconn.edu

† richard.t.jones@uconn.edu

[1] A. Dzierba et al., *The science of quark confinement and gluonic excitations*, GlueX/Hall D Design Report Version 4 (2002), available from http://www.gluex.org.

[2] R. Brun, F. Bruyant, M. Maire, A. McPherson, and P. Zanarini, *GEANT3 user's guide*, CERN report CERN-DD/EE/84-1 (1986), URL http://wwwinfo.cern.ch/asdoc/geant_

html3/geantall.html.

[3] A. Snyder, *Gelhad in bbsim*, web document (1995), package available from Hall D cvs repository, URL http://www.slac.stanford.edu/BFROOT/www/Computing/Offline/Simulation/gelhad.html.

[4] R. Jones, *HDDS - Hall D detector specification*, Hall D Technical Note (2001), URL http://zeus.phys.uconn.edu/halld/geometry/.